https://doi.org/10.5194/egusphere-2026-2016
Preprint. Discussion started: 10 July 2026

Behavioral feedbacks reshape blue–green water scarcity and sustainability trade-offs in irrigated agriculture: A sociohydrological perspective

Youzhen Lu[1], B. Shengqian Zhang[1], Mengyang Wu[1], Jan F. Adamowski[2], Xinchun Cao[1,2]

[1] College of Agricultural Science and Engineering, Hohai University, Nanjing, 210098, China
[2] Department of Bioresource Engineering, Faculty of Agricultural & Environmental Sciences, McGill University, Québec H9X 3V9, Canada

Correspondence to: Xinchun Cao (caoxinchun@hhu.edu.cn)

Abstract. Blue–green water scarcity in irrigation districts is influenced by both hydrological processes and farmer management, yet most studies treat agricultural decision-making as exogenous and static. We develop a spatially explicit, bidirectionally coupled framework integrating Soil and Water Assessment Tool (SWAT) with an agent-based model (ABM) of boundedly rational farmers, embedding crop choice and irrigation scheduling within basin-scale hydrology and crop growth. Applied to the Yaohekou Irrigation District in the Han River Basin, China, the model quantifies how behavioral heterogeneity and management portfolios affect blue–green water use, irrigation supply adequacy, ecological-flow pressure, and equitable water access in the water–ecology–food–society (WEFS) nexus. The district shows persistent supply–demand gaps and strong sensitivity to behavior. Profit-driven regimes concentrate cropping and synchronize irrigation during critical stages, increasing dry-year peak blue-water withdrawals, shrinking safety margins, and amplifying drought-time deficits and inequity. Conservative social-learning regimes maintain crop diversity and stagger demand, buffering drought impacts. Policy experiments show that supply augmentation alone is partly absorbed by demand catch-up (diminishing returns); uniform water-price increases raise efficiency but reduce equity via heterogeneous responses; combining efficiency improvements with moderate supply support lowers water use per unit output and dampens sensitivity during wet-to-dry transitions. Overall, sustainable management should target the chain of demand synchronization, peak extraction, and constraint triggering, supported by technology diffusion and protective mechanisms to build socially inclusive resilience.

1 Introduction

Under increasing hydroclimatic variability and rising agricultural production demands, the central challenge for irrigated agriculture is no longer simply “having enough water,” but how limited water resources are dynamically allocated among food production, ecological flow requirements, and spatial equity(Qi et al., 2022; Yin et al., 2024). The blue–green water framework provides a process-based lens for diagnosing these coupled pressures. Blue water refers to surface and groundwater withdrawals used for irrigation, whereas green water is rainfall-derived soil moisture consumed by crops through evapotranspiration(Hoekstra, 2019). Distinguishing these sources clarifies how crop production depends on precipitation versus managed withdrawals, and it connects field-scale decisions to basin-scale hydrologic and ecohydrologic response(Cao

https://doi.org/10.5194/egusphere-2026-2016
Preprint. Discussion started: 10 July 2026

et al., 2020; Tuninetti et al., 2015; Zhuo et al., 2014). Because ecological flow requirements are typically expressed through discharge thresholds, the magnitude and timing of blue-water withdrawals can affect the frequency and severity of ecological flow deficits(Scott et al., 2014). At the same time, access to blue water is mediated by infrastructure and institutions, making equity an intrinsic dimension of blue–green water scarcity in irrigation systems(Hassan et al., 2023; Seigerman et al., 2023).

A large body of work has quantified blue–green water consumption across scales. Field experiments have measured crop water use and yield responses under different irrigation schedules and technologies(Wu et al., 2022). Basin-scale assessments have used process-based hydrologic and crop models, such as the Soil and Water Assessment Tool (SWAT) and AquaCrop, to represent soil moisture dynamics, evapotranspiration, and irrigation requirements, and to map spatial patterns of blue and green water use(Luan et al., 2018; Zhuo et al., 2022). Regional and global syntheses have further documented where and when agricultural production depends most strongly on blue water withdrawals(Albers et al., 2021; Cao et al., 2023; Mialyk et al., 2024). A key methodological limitation nevertheless persists: agricultural management is commonly prescribed as exogenous and time-invariant (fixed cropping patterns, irrigation rules, and management intensity), thereby assuming that blue–green water dynamics respond in an approximately linear way to climate, soils, and infrastructure(Chatterjee et al., 2024). In reality, irrigation-district hydrology is co-produced by biophysical constraints and farmer decision-making(Mijic et al., 2024). Farmers respond to climate information (e.g., perceived drought risk), profit expectations, and policy signals (e.g., allocation rules, water pricing, and technology programs)(Yuan et al., 2021). Small adjustments in crop choice, irrigation depth, and irrigation timing can aggregate into basin-scale patterns that static parameterizations cannot capture(Wescoat Jr. et al., 2018). Neglecting such bottom-up behavioral feedbacks can obscure spatiotemporal heterogeneity and nonlinear interannual responses that cannot be inferred from biophysical drivers alone(Du et al., 2020).

Meanwhile, a growing body of work in agricultural economics and rural sociology has examined farmer decision-making under risk, price volatility, and institutional interventions, often formalizing behavior as expected-utility maximization or related bounded-rationality heuristics(Alam et al., 2022). Together, these studies provide multiple lenses for understanding heterogeneous farmer behavior across socioeconomic conditions and policy environments(Bourceret et al., 2022). Agent-based modeling (ABM) has become a prominent tool in this line of research because it can represent heterogeneous actors, local interactions, and adaptive dynamics(Ng et al., 2014; Nouri et al., 2019), and it is increasingly used to explore irrigation behavior and policy performance. For example, previous studies have simulated farmers' irrigation decisions and bidding strategies in a double-auction water-rights market, evaluated how taxes and subsidies shape technology adoption, and characterized livelihood adaptation under drought stress(Du et al., 2017; Duan et al., 2024; Huber et al., 2023; Wens et al., 2020) . However, many ABM studies remain weakly connected to process-based hydrologic or crop models. Without physically consistent, time-varying feedbacks from soil moisture, streamflow, and allocation constraints, it is difficult to quantify how behavioral change translates into basin-scale water cycling outcomes, including blue–green partitioning and ecohydrologic impacts.

Socio-hydrology and coupled human–natural systems (CHANS) research aims to bridge this gap by explicitly representing two-way feedbacks between human systems and hydrologic processes and by focusing on coevolutionary dynamics(Genova and Wei, 2023; Nozari et al., 2024; Sousa et al., 2025; Yoon et al., 2021). For instance, Studies show that projections neglecting

https://doi.org/10.5194/egusphere-2026-2016
Preprint. Discussion started: 10 July 2026

farmers' adaptive responses can overestimate future water scarcity(Yoon et al., 2024). These insights motivate unified frameworks that integrate process-based hydrology and crop growth with behaviorally driven decision-making, enabling dynamic assessments of blue–green water trajectories and their ecological and social consequences under changing climate and policy conditions(Filatova et al., 2025; Lyu et al., 2024).

Building on this perspective, we develop a spatially explicit, bidirectionally coupled SWAT–ABM framework that embeds boundedly rational farmer decisions (crop choice and irrigation management) into basin-scale hydrology and crop growth simulations. Using blue–green accounting, we evaluate irrigation supply gaps, ecological flow stress, and the equity of water availability as jointly determined outcomes of behavior, policy, and hydroclimate. We demonstrate the framework in the Yaohekou Irrigation District in the Han River Basin, China.

This study addresses three mechanistic questions: (1) Do behavioral differences reshape cropping patterns and irrigation timing in ways that increase demand overlap or spatial concentration, thereby amplifying dry-year blue-water deficits and ecological stress? (2) Through what behavioral–hydrologic pathways do supply augmentation, efficiency improvements, and price regulation affect system outcomes, and how do these effects depend on hydroclimatic conditions and farmer heterogeneity? (3) Under explicit ecological and equity objectives, which intervention portfolios are most likely to increase robustness to hydroclimatic variability?

Our contributions are threefold. First, we provide a reproducible SWAT–ABM coupling framework to quantify behavioral feedbacks on blue–green water use, irrigation-demand peaks, and the triggering of ecohydrologic constraints. Second, through behavioral and policy experiments, we identify how changes in demand timing and spatial allocation shape trade-offs among productivity, ecological protection, and equity across hydroclimatic regimes. Third, we translate these mechanisms into transferable diagnostic insights to support integrated blue–green water management in irrigation districts facing increasing climate variability and multi-sector competition.

https://doi.org/10.5194/egusphere-2026-2016
Preprint. Discussion started: 10 July 2026

2 Materials and Methods

2.1 Overview of the ABM-SWAT model

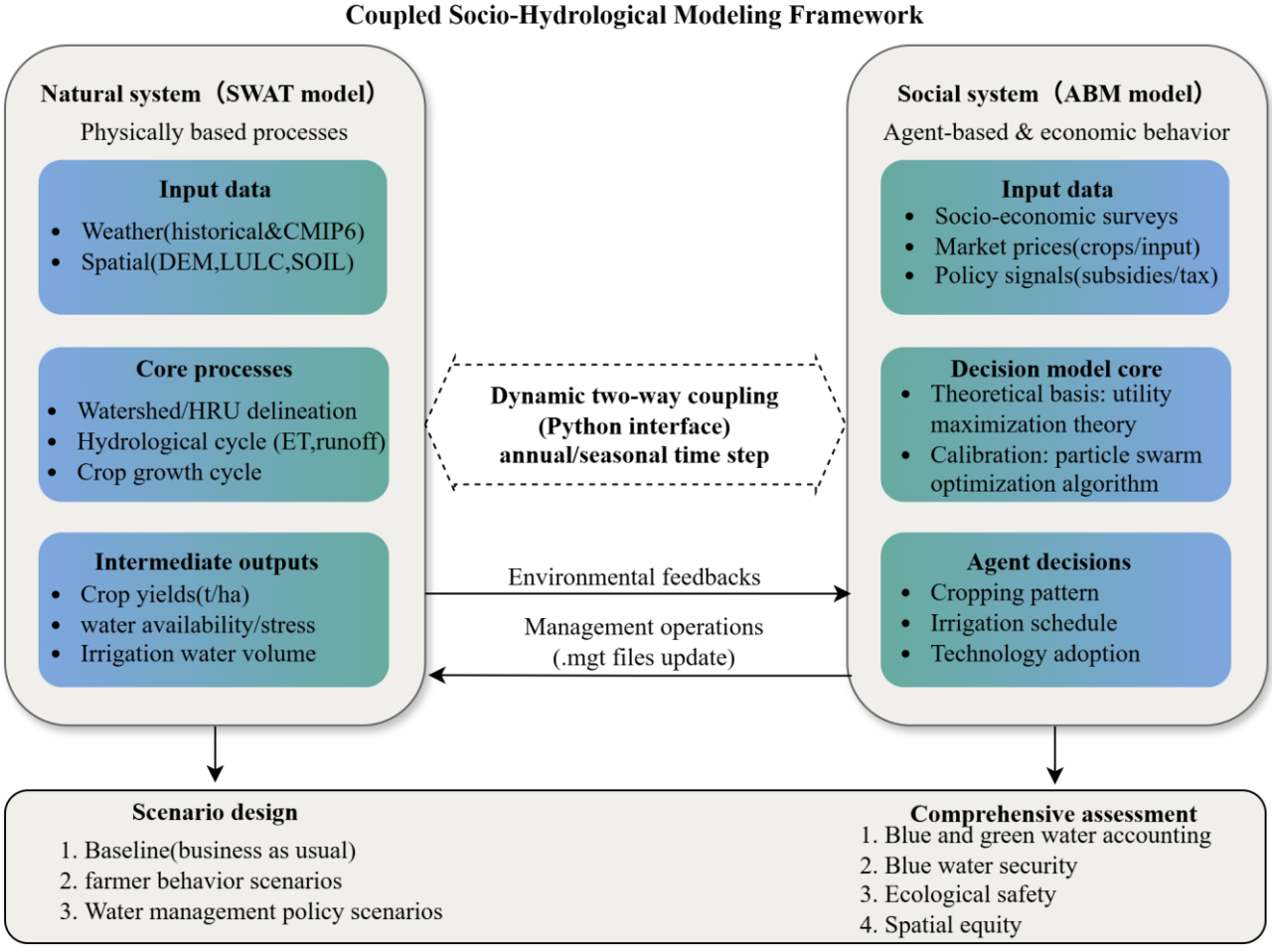

Figure 1: Model Coupling Framework

To capture feedbacks between hydrologic processes and human decision-making, we developed a coupled ABM–SWAT modeling framework with two core components: (i) the Soil and Water Assessment Tool (SWAT), which simulates basin hydrology and crop growth, and (ii) an agent-based model (ABM), which represents farmers' decision-making under uncertainty. The two components interact dynamically. SWAT provides the ABM with physically based signals describing local conditions (e.g., soil moisture and realized yield), while the ABM returns management actions (e.g., crop choice and irrigation scheduling) that update SWAT management inputs and, in turn, alter subsequent hydrologic and crop-growth trajectories.

https://doi.org/10.5194/egusphere-2026-2016
Preprint. Discussion started: 10 July 2026

2.1.1 Development of the Agent-Based Model

The ABM represents heterogeneous farmers within the CONSUMAT framework to capture bounded rationality under cognitive constraints and environmental uncertainty(Grimm et al., 2024). Unlike standard optimization approaches that assume complete information and globally optimal choices, farmers in the model adjust their decision rules dynamically as their perceived environment and psychological state evolve over time. In each year, each agent determines a management strategy consisting of spring crop choice, irrigation technology, and irrigation depth.

The decision process begins with environmental perception. Rather than responding directly to objective water availability, agents form a perceived water availability by combining external meteorological forecasts with internally formed risk perceptions. This cognitive filtering process is expressed as:

$$W_{\mathrm{per,i}}^{t} = \beta_i \cdot W_{forecast,i}^{t} + (1-\beta_i) \cdot W_{risk,i}^{t}(a_i) \quad (1)$$

where $W_{per,i}^{t}$ is the perceived water availability of agent i in year t, $W_{forecast,i}^{t}$ denotes forecast-based water information, $W_{risk,i}^{t}$ represents the agent's risk-adjusted expectation derived from historical precipitation, β_i is the forecast-trust parameter, and α_i controls the degree of risk perception, implemented as a selected quantile of the historical precipitation distribution (i.e., the corresponding quantile of a truncated normal distribution)(Yuan et al., 2021) This perceived water signal serves as the environmental input for subsequent behavioral evaluation and decision-making.

Based on perceived environmental conditions and realized outcomes, each agent then updates two psychological indicators, satisfaction and uncertainty. Satisfaction reflects the extent to which realized utility meets the agent's aspiration level and is defined as:

$$S_i^t = \frac{\pi_i^t}{\bar{\pi}^t} \quad (2)$$

where π_i^t is the realized profit of agent i in year t, and $\bar{\pi}^t$ is the average profit of all farmers in the irrigation district. Uncertainty captures the mismatch between expected and realized outcomes and is updated as:

$$U_i^t = \lambda U_i^{t-1} + (1-\lambda)\left|\pi_{i,exp}^t - \pi_{i,real}^t\right| \quad (3)$$

where $\pi_{i,exp}^t$ and $\pi_{i,real}^t$ denote expected and realized profit, respectively, and λ is a memory-decay parameter representing the persistence of previous uncertainty.

The two indicators jointly determine the farmer's behavioral state. Following the CONSUMAT logic, agent i is classified into one of four decision modes according to agent-specific satisfaction and uncertainty thresholds, γ and δ:

$$State_i^t = \begin{cases} repetition, S_i^t \geq \gamma, U_i^t < \delta \\ deliberation, S_i^t < \gamma, U_i^t < \delta \\ social\ comparison, S_i^t < \gamma, U_i^t \geq \delta \\ imitation, S_i^t \geq \gamma, U_i^t \geq \delta \end{cases} \quad (4)$$

These four states represent habitual persistence, deliberate optimization, strategy adjustment through comparison with more successful peers, and reliance on socially learned or remembered strategies under uncertainty, respectively.

https://doi.org/10.5194/egusphere-2026-2016
Preprint. Discussion started: 10 July 2026

Once the behavioral state is identified, the agent determines a decision vector $D_i^t = \{c_i^t, k_i^t, I_i^t\}$, where c_i^t, k_i^t, and I_i^t denote crop choice, irrigation technology, and irrigation depth, respectively. In general, decision-making can be written as

$$D_i^t = \Phi\left(State_i^t, W_{per,i}^t, X_i^t\right) \quad (5)$$

where X_i^t denotes the agent's production and resource conditions. Under repetition, the agent retains the previous crop and irrigation technology while re-optimizing irrigation depth for current conditions. Under deliberation, crop choice, irrigation technology, and irrigation depth are jointly re-optimized. Under social comparison, the agent evaluates the strategic package adopted by a higher-performing neighbor and adopts it if it improves expected utility, after which irrigation depth is optimized. Under imitation, the agent recalls or samples a socially available strategy and retains it when it is expected to perform better than the current one, with irrigation depth subsequently optimized. The full mathematical formulation of the rolling-horizon optimization model, including the objective function, water–yield relationship, and associated constraints, is provided in Supplementary material.

2.1.2 Hydrology–Crop Model

Basin hydrologic processes and crop growth were simulated using the Soil and Water Assessment Tool (SWAT). The watershed was discretized into hydrologic response units (HRUs), which serve as the fundamental computational units for representing spatial heterogeneity(Luan et al., 2018; Xiong et al., 2019). SWAT's land-phase hydrology is driven by a daily soil-water balance, which tracks precipitation inputs, infiltration, evapotranspiration, runoff, percolation, and lateral flow.

This process representation enables explicit attribution of crop water use to green water versus blue water. Irrigation is simulated as a dynamic blue-water abstraction from an aquifer or surface-water source to satisfy crop water requirements and replenish soil moisture. Potential evapotranspiration was estimated using the Penman–Monteith method. Crop growth is tightly coupled to the water balance and is simulated using heat-unit accumulation to represent phenological development. Water stress, quantified as the deficit between potential crop water demand and actual plant water uptake, directly constrains biomass accumulation and reduces final yield(Xu et al., 2019).

To enable dynamic interaction with the agent-based model, the SWAT source code was further modified so that the model could receive externally generated management inputs during simulation, including agent-specific decisions on crop choice, irrigation technology, irrigation scheduling, and irrigation amount. These additions were implemented by introducing customized functions into the SWAT source code to read and update management operations from external files rather than relying solely on predefined static management schedules. After incorporating these modifications, the source code was recompiled to generate a customized executable file for the coupled SWAT–ABM simulations. In this way, the hydrology–crop model responded not only to meteorological and soil conditions, but also to dynamically updated human management decisions. Additional details on the SWAT setup and model modifications are provided in Supplementary material.

https://doi.org/10.5194/egusphere-2026-2016
Preprint. Discussion started: 10 July 2026

2.1.3 Model Coupling

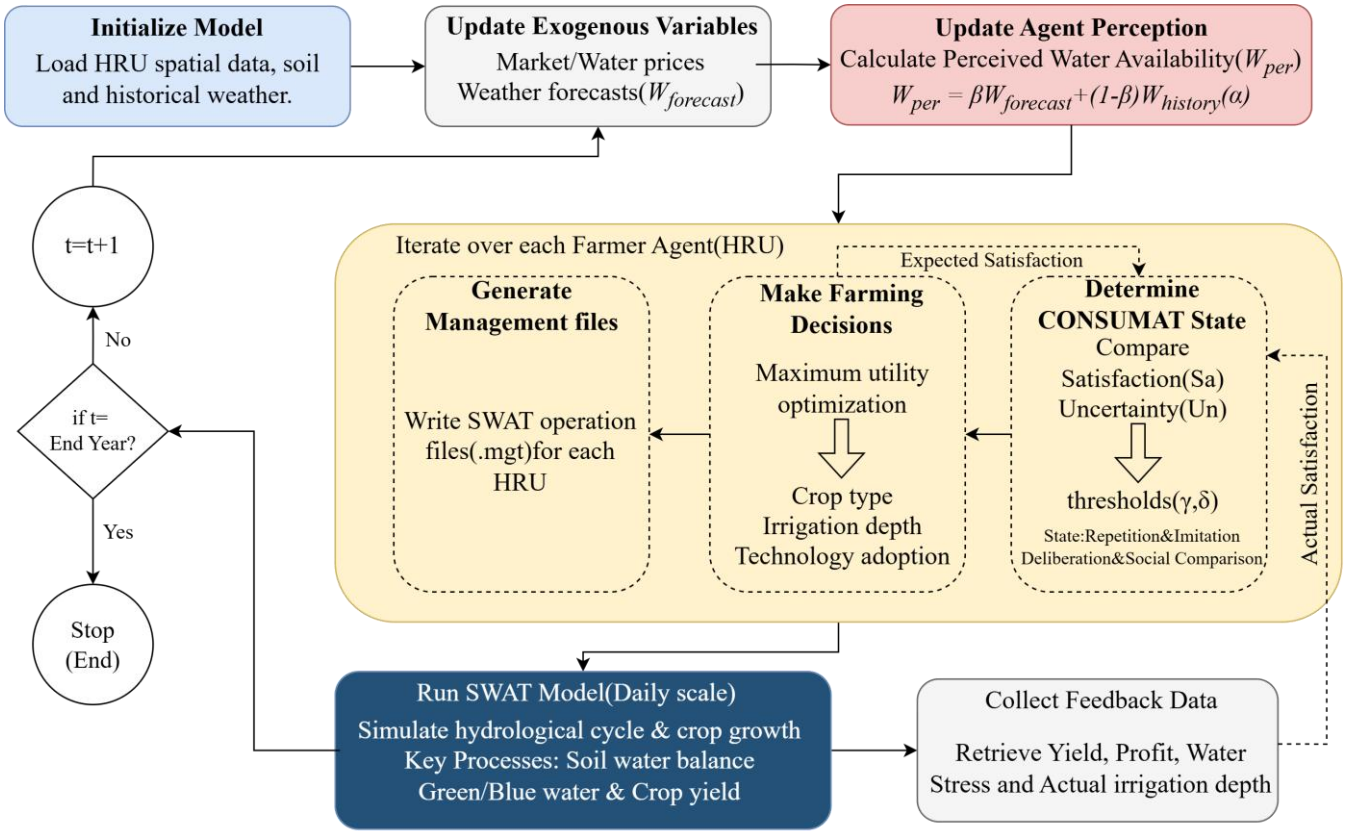

Figure 2: Model Coupling Framework

The ABM and SWAT were integrated through a Python-based coupling framework that synchronizes SWAT's daily hydrologic time step with the farmers' annual decision cycle (Fig. 2). During the initialization stage, the SWAT model discretizes the watershed into hydrologic response units (HRUs), and HRUs classified as agricultural land are assumed to correspond to individual farmer agents in the ABM. At the start of each simulation year, agents update perceived water availability using current exogenous information (e.g., seasonal climate forecasts). Importantly, each agent's behavioral state for year t is determined by the satisfaction and uncertainty values carried over from the end of year t–1. Given the resulting state, the agent selects annual management actions (e.g., crop type and irrigation depth). In states involving more deliberate evaluation (notably deliberation), agents compute an expected satisfaction based on expected utility.

The Python interface then translates these agent decisions into SWAT inputs by dynamically updating the management files (.mgt) associated with each HRU. SWAT is subsequently executed at a daily time step for the full year. After the run, physical outputs (e.g., yield and profit) are extracted to compute realized satisfaction. Uncertainty for the next cycle is updated as the absolute deviation between expected satisfaction (formed at the decision stage) and realized satisfaction (observed at year end). This feedback closes the decision–hydrology loop and governs the agent's behavioral state in the subsequent year.

https://doi.org/10.5194/egusphere-2026-2016
Preprint. Discussion started: 10 July 2026

2.2 Green-Blue Water Accounting and Assessment Framework

To systematically evaluate the water resources system, we developed an integrated methodological framework. This framework first quantifies the physical flows of green and blue water based on the SWAT model, and subsequently constructs a multi-dimensional index system to assess blue-water security, ecological safety, and spatial equity.

2.2.1 Green and Blue Water Accounting

To distinguish between green and blue water contributions within the soil profile, we implemented a daily soil water balance tracking algorithm based on the outputs of the SWAT model. The algorithm is grounded in the principle of mass conservation, where the total soil water content (SW_t,mm) at any time step is the sum of the green ($SW_{green,t}$,mm) and blue ($SW_{blue,t}$,mm) water storage(Hoekstra, 2019; Li et al., 2024; Zhuo et al., 2016). The dynamics of these storage components are described by Eq. (6):

$$\begin{cases} SW_t = SW_{t-1} + W_{in,t} - L_{out,t} \\ SW_{green,t} = SW_{green,t-1} + W_{in,t} \times \frac{PRECIP_t}{RECIP_t + IRR_t} - L_{out,t} \times \frac{SW_{green,t-1}}{SW_{t-1}} \\ SW_{blue,t} = SW_{blue,t-1} + W_{in,t} \times \frac{IRR_t}{PRECIP_t + IRR_t} - L_{out,t} \times \frac{SW_{blue,t-1}}{SW_{t-1}} \end{cases} \quad (6)$$

Where $W_{in,t}$ represents the effective infiltration entering the soil profile, and $L_{out,t}$ denotes the total water loss from the soil profile. These fluxes are defined as:

$$\begin{cases} W_{in,t} = PRECIP_t + IRR_t - SURQ_t \\ L_{out,t} = ET_t + PERC_t + LATQ_t \\ ET_{green} = ET_t \times \frac{SW_{green,t-1}}{SW_{t-1}} \\ ET_{blue} = ET_t \times \frac{SW_{blue,t-1}}{SW_{t-1}} \end{cases} \quad (7)$$

As shown in the equations, the partitioning follows a proportional mixing assumption. The effective infiltration ($W_{in,t}$) is allocated to green or blue water storage based on the ratio of precipitation ($PRECIP_t$) to irrigation (IRR_t) on the current day. Conversely, the outflows ($L_{out,t}$), which include evapotranspiration (ET_t), percolation ($PERC_t$), and lateral flow ($LATQ_t$), are assumed to remove water from the soil in proportion to the mixed ratio of green and blue water present in the soil at the previous time step (t-1). Finally, the green and blue components of actual evapotranspiration (ET_{green} and ET_{blue}) are derived based on this updated storage composition.

2.2.2 Construction of Multi-dimensional Assessment Indices

The Blue Water Deficit Index (BDI) measures irrigation supply adequacy, defined as the share of blue-water requirement that is met. Theoretical blue water requirement ($D_{b,req}$) was defined as the difference in crop evapotranspiration between a no-stress auto-irrigation scenario ($ET_{optimal}$) and a rainfed scenario (ET_{rain}). The index is calculated as:

https://doi.org/10.5194/egusphere-2026-2016
Preprint. Discussion started: 10 July 2026

$$\begin{cases} D_{b,req,t} = ET_{optimal,t} - ET_{rain,t} \\ BDI_t = 1 - \frac{D_{b,req,t} - ET_{blue,actual,t}}{D_{b,req,t}} \end{cases} \quad (8)$$

Where $ET_{blue,actual}$ represents the actual blue water consumption. The BDI ranges from 0 to 1, where a value of 1 indicates no deficit (supply fully meets demand), while values approaching 0 indicate severe shortage.

The Ecological Blue Water Stress Index (WSI_{eco})quantifies the ecological stress on river ecosystems by measuring the extent to which ecological flow requirements are unmet. It is defined as the ratio of the ecological flow deficit to the total requirement (Q_{eco})(Ding et al., 2024).

$$WSI_{eco} = \frac{max(Q_{eco,t} - Q_{out,t}, 0)}{Q_{eco,t}} \quad (9)$$

Where $Q_{out,t}$is the simulated streamflow. The index ranges from 0 to 1, where a value of 0 indicates a healthy state (flow requirement fully met), while values approaching 1 indicate critical ecological stress (river drying or severe flow depletion).

To evaluate spatial equity in irrigation water accessibility, we developed the Blue-water Availability Equity Index ($BAEI$)based on the Gini coefficient of the across sub-basins. To account for varying irrigation scales, the calculation is weighted by the irrigation area (ω) of each sub-basin. The index is defined as the complement of the spatial Gini coefficient (G_{space}):

$$BAEI = 1 - G_{space} = 1 - \frac{\sum_{i=1}^{n}\sum_{j=1}^{n}\omega_i\omega_j|BDI_i - BDI_j|}{2\mu(\sum_{i=1}^{n}\omega_i)^2} \quad (10)$$

Where$\mu$is the area-weighted mean BDI.The $BAEI$ ranges from 0 to 1, where a value of 1 indicates perfect spatial equity, while lower values denote significant disparity in water scarcity distribution.

https://doi.org/10.5194/egusphere-2026-2016
Preprint. Discussion started: 10 July 2026

2.3 Study area and Data sources

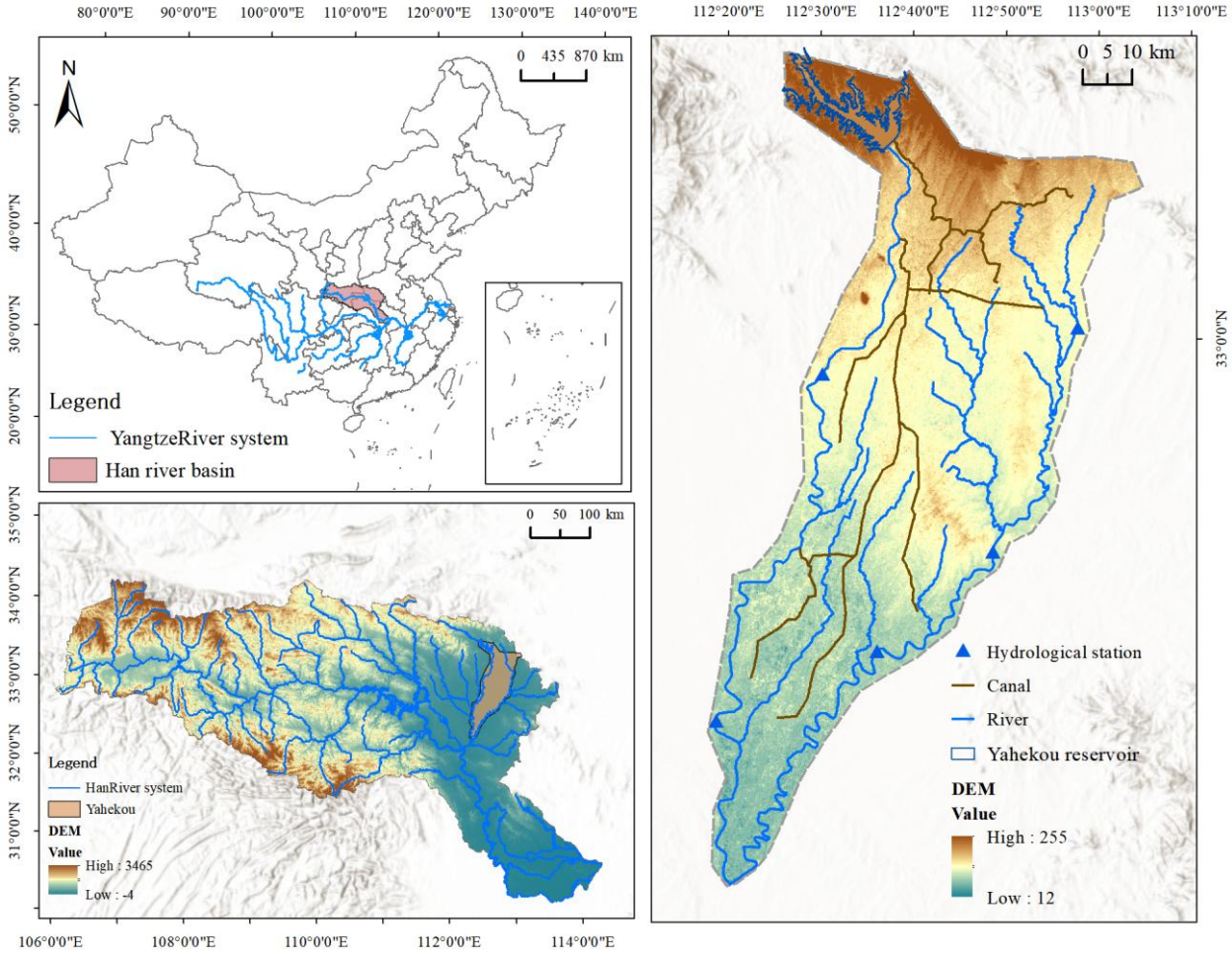

Figure 3: Study Area

The Yaohekou Irrigation District is located in the Han River Basin, Henan Province, China (112°39′E–112°54′E, 32°27′N–33°09′N). The terrain slopes from north to south (approximately 160–80 m a.s.l.), and irrigation is supplied through a gravity-fed conveyance system supported by the multi-year regulating Yaohekou Reservoir (total storage 13.39 × 10^8 m³). The region has a subtropical monsoon climate with mean annual precipitation of 802.7 mm, more than 63% of which falls during June–September. This strong seasonality creates a recurrent mismatch between water supply and agricultural demand in winter and spring. Soils are dominated by Vertisols, characterized by heavy texture and high water-holding capacity but low permeability, which increases crop sensitivity to irrigation timing and management intensity. Cropping follows a typical double-cropping rotation: winter wheat followed by spring/summer crops dominated by maize, peanut, and soybean. The district faces multiple water-resource tensions. Peak agricultural irrigation demand in spring–summer can compete with ecological baseflow

https://doi.org/10.5194/egusphere-2026-2016
Preprint. Discussion started: 10 July 2026

requirements, while municipal and industrial water demands are also supplied by the reservoir, intensifying multi-sector competition for regulated releases. In addition, conveyance and allocation through the canal network can create spatial gradients in water accessibility (e.g., differences in reliability and delivery timing along the network), which may promote spatial concentration of blue-water use and uneven distribution of scarcity impacts. Detailed crop management practices and the spatial and time-series datasets (sources and resolutions) are provided in Supplementary material.

2.4 Model calibration and validation

We adopted a stepwise calibration and validation strategy for the coupled SWAT–ABM framework in order to constrain both its biophysical and behavioral components. Because the observed dynamics of the irrigation district reflect the combined effects of hydrological forcing and farmer management, different observational datasets were used to calibrate different parts of the model rather than treating all system responses as purely physical outputs.

2.4.1 Hydrological calibration and validation

The SWAT component was first calibrated to provide a physically credible basis for the coupled simulations. This step was necessary because the ABM relies on SWAT-generated environmental signals, including soil water conditions, crop water stress, and realized yields, to update farmer perceptions, satisfaction, and subsequent decisions. Sensitivity analysis and parameter calibration were conducted using the SUFI-2 algorithm implemented in SWAT-CUP(Abbaspour et al., 2015). Observed runoff data from five hydrological stations within the basin were used, with 2007–2010 as the calibration period and 2011–2013 as the validation period. Model performance was evaluated using the Nash–Sutcliffe efficiency (NSE), the coefficient of determination (R^2), and percent bias (PBIAS). Following commonly used criteria, performance was considered satisfactory when $NSE > 0.5$, $R^2 > 0.6$, and $|\ PBIAS\ | < 25\%$(D. N. Moriasi et al., 2007). The calibration and validation results for the five stations are summarized in Table 1, indicating that the model reproduced the main magnitude and temporal variability of runoff across the monitoring network. The calibrated SWAT parameters and the comparison between observed and simulated runoff are provided in Supplementary material.

Table 1 Model Performance during calibration (2007–2010) and validation (2011–2013).

Observation point/data	Calibration period (2007-2010)			Validation period (2011-2013)		
	R^2	NSE	PBIAS%	R^2	NSE	PBIAS
Nanyang Station	0.82	0.74	-20	0.76	0.69	-22
Xindianpu Station	0.88	0.84	22	0.64	0.59	19
Sheqi Station	0.78	0.82	-16	0.73	0.68	-6
Tanghe Station	0.69	0.67	18	0.66	0.63	13

https://doi.org/10.5194/egusphere-2026-2016
Preprint. Discussion started: 10 July 2026

Guotan Station	0.72	0.69	22	0.69	0.55	19

2.4.2 Behavioral parameter calibration and validation

Hydrological calibration alone cannot constrain observed changes in cropping structure or irrigation withdrawals, because these emerge from farmer decisions rather than from biophysical forcing alone. We therefore calibrated the key behavioral parameters of the coupled model using two aggregated indicators of farmer activity: observed crop planting area and total canal-head diversion. Crop planting area was used to constrain the collective outcome of crop-choice decisions, whereas canal-head diversion was used to constrain the aggregate irrigation demand generated by farmer management under limited water supply.

The behavioral calibration focused on four parameters, $(\alpha, \beta, \gamma, \delta)$, which govern farmer cognition and adaptive response in the ABM. Specifically, αrepresents risk perception, βdenotes trust in climate forecasts, and $\gamma$and δcontrol the switching sensitivity among CONSUMAT behavioral states. Because micro-level socioeconomic observations were not available for individual farmers, these parameters were estimated using particle swarm optimization (PSO) (James V. Miranda, 2018). The swarm size was set to 10, and initial parameter values were uniformly sampled from [0,1]. The objective function was defined as the weighted sum of the mean square errors (MSE) for crop planting area and canal-head diversion. The resulting optimal parameter set was used as the baseline behavioral configuration for the subsequent scenario experiments.

The calibrated values of the four behavioral parameters, together with the corresponding fitting errors for crop planting area and canal-head diversion, are summarized in Table 2. The relatively small differences between calibration and validation errors indicate that the calibrated parameter set provides a stable representation of farmer decision-making at the aggregate level.

Table 2 Calibrated behavioral parameter values and corresponding fitting performance for crop planting area and canal-head diversion

Item	Description	Calibration (2007-2010)	Validation (2011-2013)
Calibrated behavioral parameters			
α	Risk-perception parameter	0.57	-
β	Forecast-trust parameter	0.58	-
γ	Behavioral switching threshold	0.27	-
δ	Behavioral switching threshold	0.023	-
Fitting performance			
MSE_{area}	Mean square error for crop planting area	0.032	0.041
$MSE_{diversion}$	Mean square error for canal-head diversion	0.051	0.055

https://doi.org/10.5194/egusphere-2026-2016
Preprint. Discussion started: 10 July 2026

Weighted objective	Weighted sum of MSEs	0.0415	0.048

2.4.3 Overall model performance and validation logic

The coupled framework was considered satisfactory only when it reproduced both observed runoff dynamics and the aggregated patterns of human-modified cropping and water withdrawal. This dual criterion is important in socio-hydrological modeling, because agreement with runoff alone does not ensure that behavioral feedbacks are realistically represented. Overall calibration and validation results are summarized in Tables 1 and 2. The hydrological component performed satisfactorily across the monitoring stations, and the coupled model also reproduced planting area and canal-head diversion with acceptable error.

To further assess whether explicit representation of farmer decision-making improves hydrological realism, we compared the validation performance of the dynamically coupled SWAT–ABM model with that of a static-management configuration at Nanyang Station, which is located immediately downstream of the irrigation intake and is therefore expected to be particularly sensitive to irrigation diversion and management operations. Relative to the static configuration, the dynamic model improved NSE from 0.69 to 0.74 and R^2 from 0.76 to 0.77, while reducing $|PBIAS|$ from 22% to 13%. These improvements indicate that incorporating time-varying farmer decisions helps the model better capture the anthropogenic regulation signal embedded in local flow dynamics. We therefore interpret the enhanced performance at Nanyang Station as supporting evidence that farmer decision-making is an important contributor to the observed hydrological state in the irrigation district

Table 3 Validation performance of the static-management and dynamic farmer-decision model configurations at Nanyang Station.

Model configuration	NSE	R^2	PBIAS (%)
Static management	0.69	0.76	-22
Dynamic farmer decisions	0.74	0.77	-13
Improvement	+0.05	+0.01	+9

2.5 Scenario Design and Simulation Experiments

Simulations were conducted for 2007–2020, with 2007 treated as a warm-up year. All experiments were designed around the calibrated baseline configuration, and only behavioral parameters or management controls were perturbed while keeping the hydrological settings unchanged.

We designed eight behavioral scenarios to examine how alternative decision mechanisms reshape blue–green water dynamics. These scenarios were organized into three groups: sensitivity scenarios, which tested the extreme effects of risk perception and forecast trust; psychological archetype scenarios, which combined high and low values of α and β to represent contrasting cognitive styles; and adaptation scenarios, which varied the behavioral switching thresholds γ and δ to test sensitivity to decision-state transitions.

https://doi.org/10.5194/egusphere-2026-2016
Preprint. Discussion started: 10 July 2026

To assess management responses, we further designed three policy scenarios representing supply augmentation, integrated efficiency improvement, and economic regulation through water pricing. For all scenarios, model outputs were evaluated as relative changes from the baseline in blue-water security, ecological stress, productivity, and equity indicators. The full scenario definitions are listed in Table 4.

Table 4 Scenario Design for behavioral parameters and Water Management Policies

Category	ID	Scenario Name	Description and Parameter Settings
Farmer Behavior			Psychological and Adaptive Attributes (α, β, γ, δ)
Reference	S0	Behavior Baseline	Calibrated (α, β, γ, δ)
Sensitivity	S1	Extreme Optimism	α=1.0
	S2	Extreme trust in forecasts	β=1.0
Psychological	S3	Conservative	α=0.2, β=0.2
	S4	Forecast-driven	α=0.2, β=0.9
	S5	Optimistic experience	α=0.9, β=0.2
	S6	Proactive Optimist	α=0.9, β=0.9
Adaptability	S7	Satisficing	γ=0.1, δ=0.01
	S8	Maximizing	γ=0.5, δ=0.3
Management Policy			Supply Limits and Economic Instruments
Baseline	M0	Policy Baseline	no intervention.
Supply-side	M1	Supply Augmentation	Irrigation water supply limit increased by +20%.
Integrated	M2	Integrated Efficiency	Supply limit +20% with enhanced conveyance efficiency (η +0.1).
Integrated	M3	Integrated Economic	Supply limit +20% with water price hike (+0.1 CNY/m^3).

https://doi.org/10.5194/egusphere-2026-2016
Preprint. Discussion started: 10 July 2026

3 Results

3.1 Spatiotemporal Evolution of Blue-Green Water and Ecological Stress under the Baseline Scenario

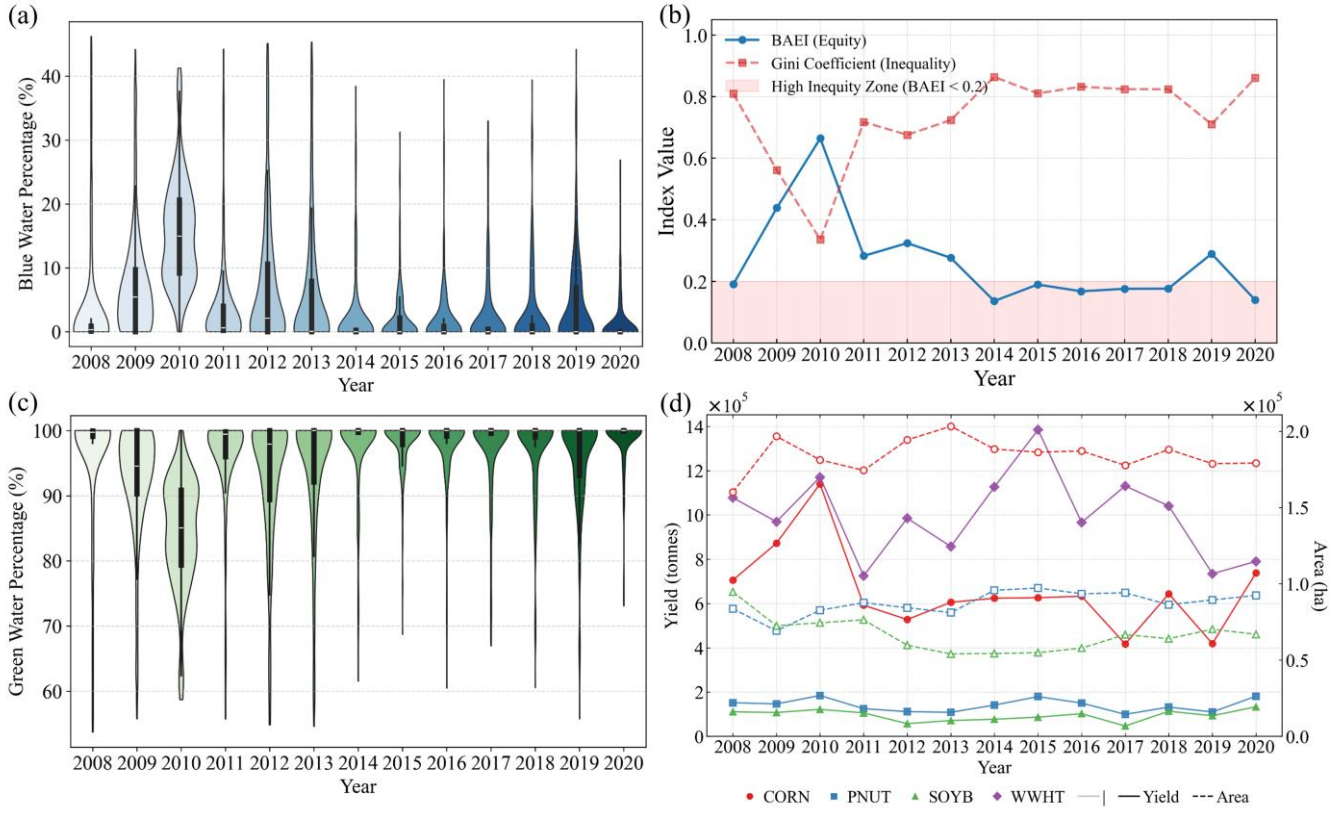

Figure 4: Baseline spatiotemporal patterns of blue–green water use, equity, and crop production (2008–2020). (a) Annual distribution of blue-water fraction across spatial units, shown as violin plots. (b) Interannual evolution of BAEI (higher values indicate greater equity) and the Gini coefficient (inequality), with the shaded band highlighting the high-inequality zone (BAEI < 0.2). (c) Annual distribution of green-water fraction across spatial units. (d) Time series of crop yields and planted areas for major crops (corn, peanut, soybean, and winter wheat); yield and area are plotted on separate axes as indicated.

Under the baseline scenario, crop water consumption is dominated by green water: the median green-water fraction exceeds 90% (Fig. 4c), indicating that agricultural production relies primarily on precipitation inputs. In contrast, blue-water consumption does not contract linearly with wetter climatic conditions, but exhibits pronounced nonlinear interannual responses. For example, in the wet year 2010, the spatial extent of blue-water consumption did not shrink; instead, it expanded and remained high (Fig. 4a). This counterintuitive pattern is consistent with two concurrent process changes. First, cropping patterns shifted slightly toward relatively water-intensive yet high-value crops, with modest increases in soybean and peanut area (Fig. 4d), thereby increasing irrigation demand from the consumption side. Second, the district's conveyance and delivery regime, characterized by continuous supply in main and branch canals and rotational delivery in lateral canals, may have lowered access barriers for headworks and near-canal users in wet years. Higher runoff supports sustained water levels in main

https://doi.org/10.5194/egusphere-2026-2016
Preprint. Discussion started: 10 July 2026

canals, making withdrawals easier for users located closer to canals and potentially inducing availability-driven water use, which would reduce the expected "wet-year" contraction of blue-water consumption. Overall, these results suggest that blue-water use is shaped not only by hydroclimatic supply, but also by management-related accessibility and crop-structure adjustments.

Beyond interannual variability, the irrigation delivery system and gradients in water accessibility also influence the spatial distribution of water stress and equity. After 2014, the basin-scale equity index (BAEI) dropped below 0.2 while the Gini coefficient remained near 0.8 (Fig. 4b), indicating substantial disparities in blue-water accessibility within the district. These disparities are closely linked to position within the conveyance network: upstream users near main and branch canal headworks typically experience higher withdrawal reliability, whereas downstream users face greater risks of delivery delays and supply uncertainty. Such accessibility gradients promote spatial concentration of blue-water consumption in high-reliability areas, thereby reinforcing uneven water-stress burdens across the irrigation district.

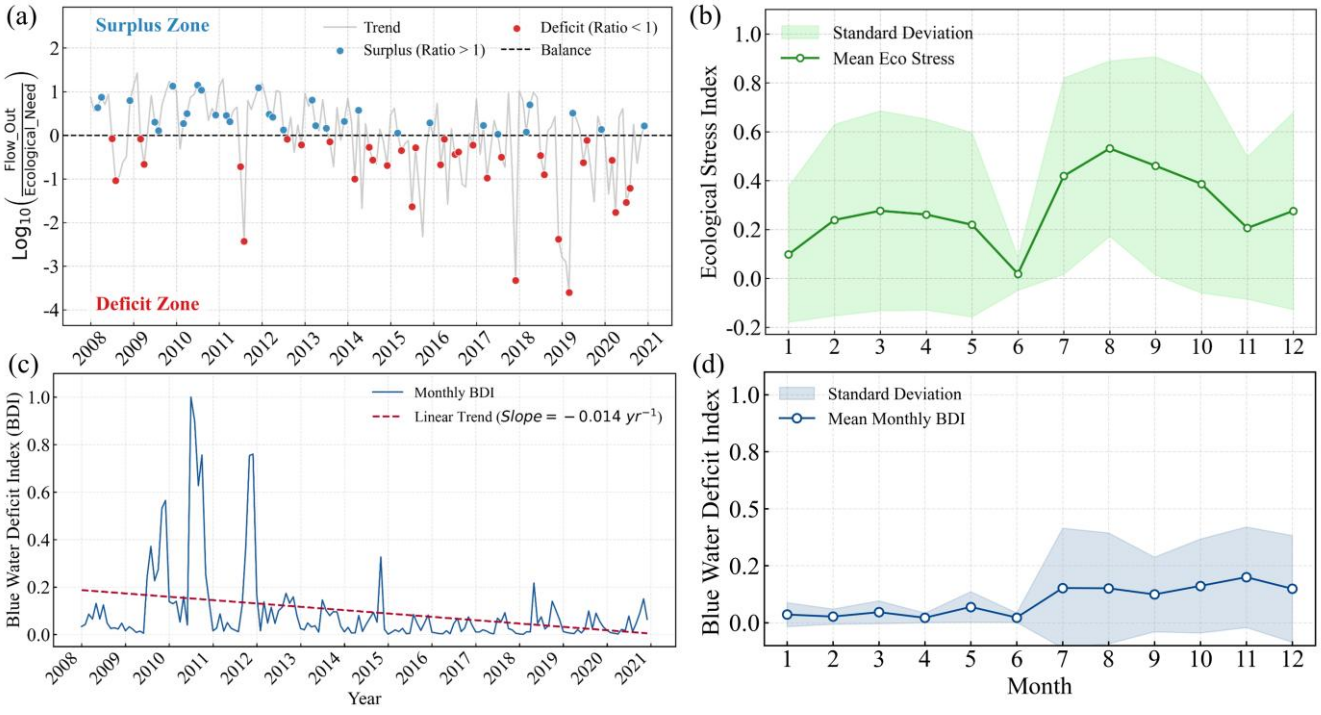

Figure 5: Baseline ecological-flow condition and irrigation blue-water deficit dynamics. (a) Interannual anomalies of river outflow relative to the ecological-flow target, expressed as log10(Flow out/Ecological need); points above zero (blue) indicate surplus (ratio > 1) and points below zero (red) indicate deficit (ratio < 1). (b) Monthly climatology of the ecological stress index, shown as the mean and variability. (c) Time series of the monthly blue-water deficit index (BDI), with the fitted linear trend (slope = −0.014 yr^{-1}). (d) Monthly climatology of BDI, showing the mean and variability.

The persistent mismatch between agricultural demand and limited water supply further manifests as coupled risks of agricultural water deficits and ecological degradation. The blue-water deficit index (BDI) shows a declining trend, and its monthly mean remains below 0.2 for much of the simulation period (Fig. 5d), indicating chronically low irrigation supply

https://doi.org/10.5194/egusphere-2026-2016
Preprint. Discussion started: 10 July 2026

satisfaction with a structural character. Consistent with this, crop yields display strong interannual variability (Fig. 4d). As the dominant crop by planted area, maize is particularly sensitive to water shortage, and yield reductions in dry years largely drive fluctuations in total agricultural production, implying that current supply reliability is insufficient to stabilize production of the primary crop. Meanwhile, river ecosystems remain under substantial stress even when irrigation satisfaction is low. Streamflow frequently falls below the ecological minimum-flow threshold (Fig. 5a), and ecological deficits become increasingly persistent after 2018. Seasonally, ecological blue-water pressure peaks in summer (index approaching 0.6; Fig. 5b), coinciding with critical water-demand periods for maize and other major crops. This overlap indicates strong competition between irrigation withdrawals and ecological baseflow during the irrigation season, making ecological constraints more likely to be triggered under dry or high-demand conditions.

https://doi.org/10.5194/egusphere-2026-2016
Preprint. Discussion started: 10 July 2026

3.2 Reshaping of Spatiotemporal Blue-Green Water Patterns by Dynamic Behavior

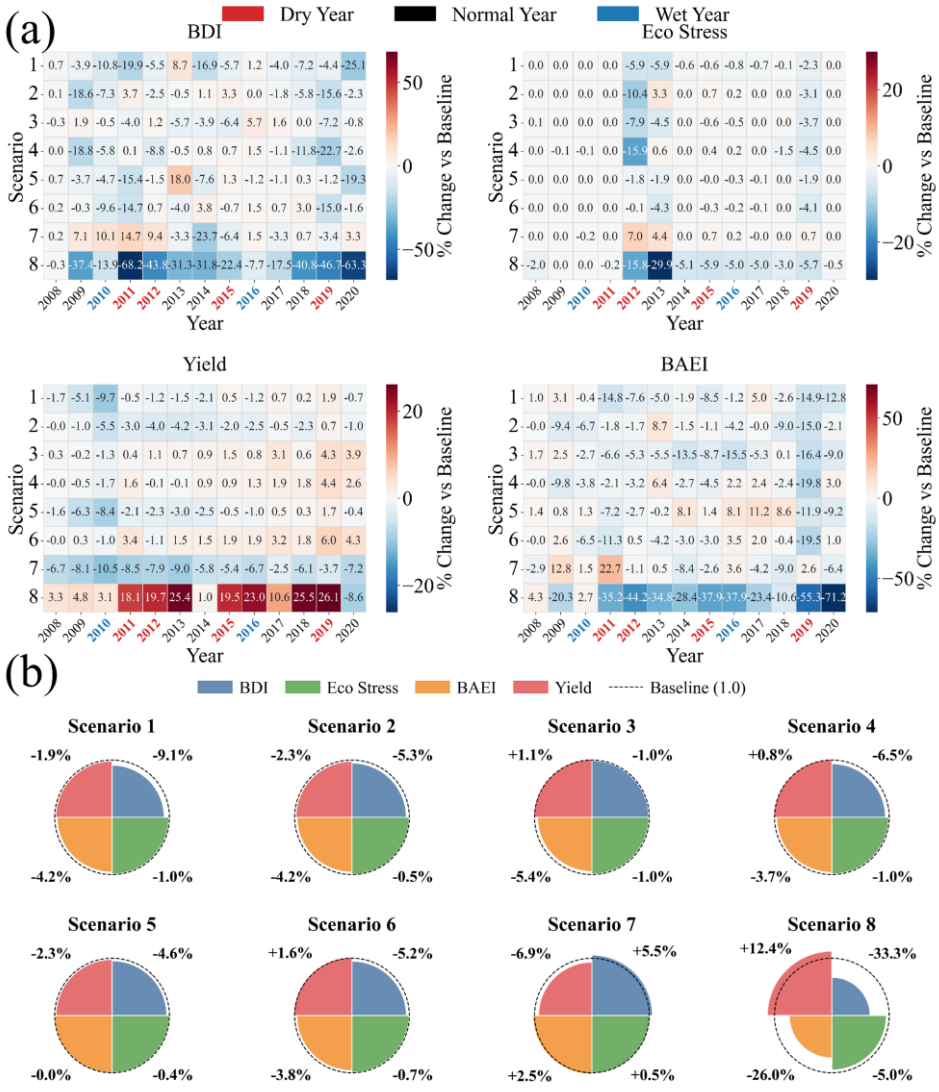

Figure 6: Behavioral-scenario impacts on basin performance relative to the baseline. (a) Heatmaps show annual percent change (%) in basin-scale blue-water security (BDI), ecological stress (WSIeco), crop yield (Yield), and allocation equity (BAEI) for eight behavioral scenarios (rows, S1–S8) over 2008–2020 (columns), expressed as changes relative to the baseline simulation. (b) Summary "score" charts synthesize mean relative changes across the simulation period for each scenario, with the dashed circle indicating the baseline (1.0).

Based on similarities in behavioral settings and simulated outcomes (Fig. 6), these scenarios can be grouped into four categories to highlight how alternative decision mechanisms restructure trade-offs among productivity, water security, equity, and ecological pressure.

The cognitive-bias and single-dependence scenarios (S1, S2, S5) exhibit a trade-off characterized by deterioration in social-system indicators alongside reduced ecological stress. Across the simulation period, yields under these scenarios are

https://doi.org/10.5194/egusphere-2026-2016
Preprint. Discussion started: 10 July 2026

generally slightly below the baseline, and dry years feature concurrent declines in both blue-water security and equity. In the severe drought of 2019, S2 shows the strongest response: BDI decreases by 15.6%, BAEI by 15.0%, and Yield by 1.0%. Notably, despite the worsening of social indicators in drought years, ecological stress does not increase; instead, it declines to varying degrees. This pattern suggests that under cognitive bias or reliance on a single information source, farmers do not follow a pathway of intensified water use to offset risk, which inadvertently preserves ecological flows; however, this comes at the expense of agricultural output and the social performance of water availability.

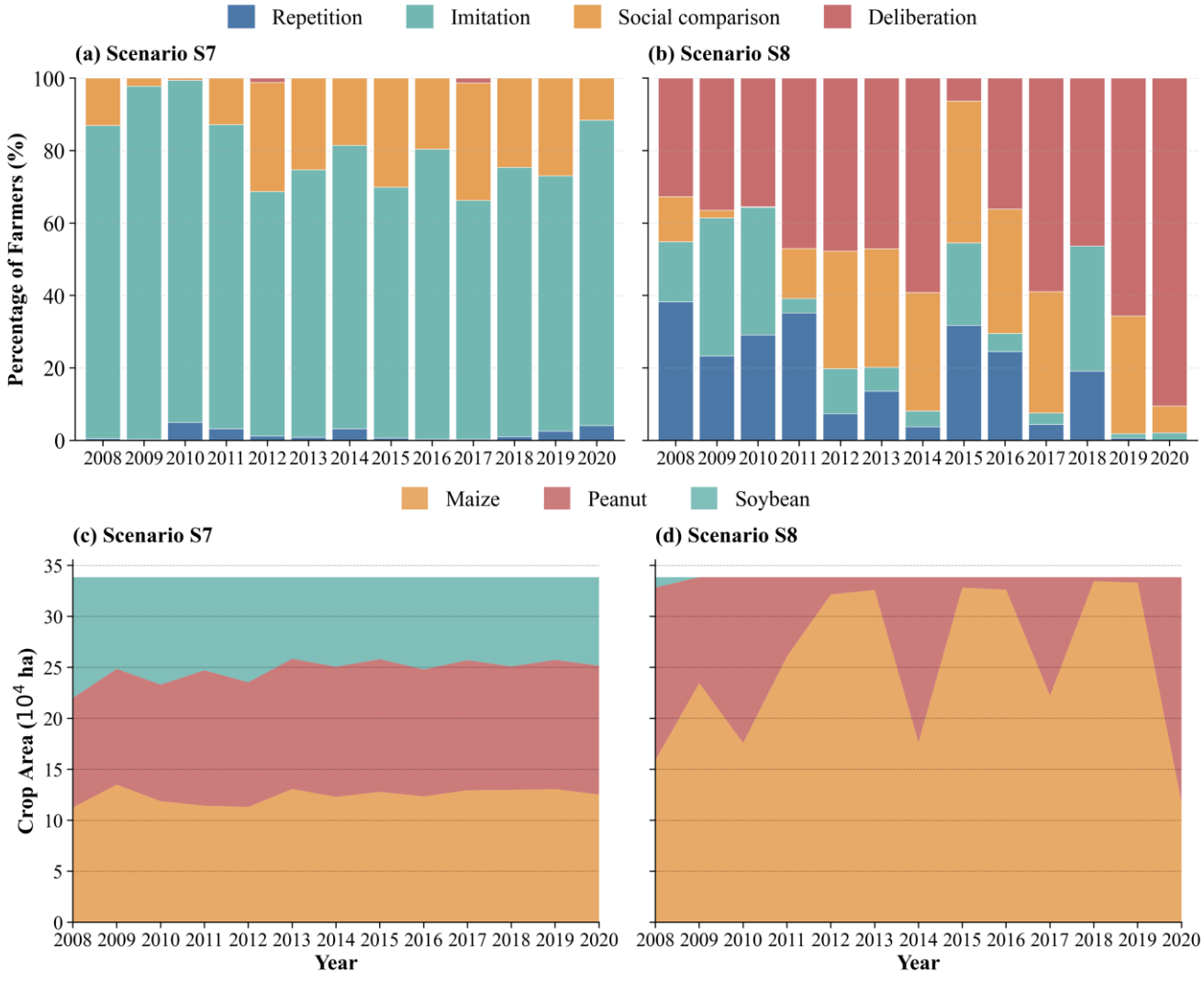

Figure 7: Behavioral-state dynamics and crop-area evolution in the contrasting adaptive scenario (a–b) Annual composition of farmer behavioral states in S7 and S8, shown as the percentage of agents operating in repetition, imitation, social comparison, and deliberation from 2008 to 2020. (c–d) Corresponding temporal evolution of planted area for major spring crop

https://doi.org/10.5194/egusphere-2026-2016
Preprint. Discussion started: 10 July 2026

In contrast, the risk-averse scenarios (S3, S4) are characterized by low-variability, defensive stability. Yield changes are small overall (typically between 0% and +1.1%), indicating that conservative decisions constrain the production ceiling while improving stability in hydrologic and ecological dimensions. In moderately dry and drought years, these scenarios dampen negative BDI fluctuations and reduce ecological stress. For example, in 2011 S3's BDI declines by only 4.0%, while in 2012 S4's ecological stress decreases by 15.9%. These results indicate that risk-averse strategies buffer dry-period constraints by limiting high-water-demand configurations and irrigation intensity, trading modest yield gains for system-level stability.

The risk-seeking scenario (S6) shows a coexistence of higher production and compressed safety margins. During the later period (2015–2020), S6 produces sustained yield increases (+1.5% to +6.0%), while ecological stress remains largely stable or slightly improves in most years. However, social-system indicators deteriorate sharply in extreme drought conditions: in 2019, BDI declines by 15.0% and BAEI by 19.5%. This contrast suggests that expansionary production driven by optimistic expectations raises output but also increases aggregate water demand and reduces the system's buffer, making supply constraints and spatial inequities more likely to emerge in dry years.

The threshold/adaptation contrast (S7 vs. S8) reveals the strongest cross-scale trade-off. S8 combines high gains with high risk: the heatmaps show widespread yield increases, including a basin-wide Yield increase of 26.1% in 2019, but with severe degradation of blue-water security and equity in the same year (BDI −46.7%, BAEI −55.3%). Decision-state outputs further show that S8 farmers more frequently enter deliberation and social comparison in drought years (Fig. 7b), consistent with convergence in cropping decisions. In pursuit of higher returns, farmers collectively shift toward drought-tolerant, high-yield maize, increasing the maize share to 98.4% in 2019 (Fig. 7d). This single-crop dominance intensifies the overlap of irrigation demand during critical growth stages, elevates basin-scale peak withdrawals, and exceeds supply capacity in dry years, thereby triggering constraints in a concentrated manner. By comparison, S7 exhibits lower yields but higher robustness: although Yield remains negatively biased (−2.5% to −10.5%), S7 is the only scenario that achieves simultaneous improvements in 2011 (BDI +14.7% and BAEI +22.7%). State analysis indicates that most S7 farmers remain in imitation (Fig. 7a), which suppresses rapid crop convergence and maintains a mixed structure of maize, peanut, and soybean (Fig. 7c). By staggering crop water-demand peaks through phenological differences, this diversity reduces demand synchronization, preserves safety margins in drought years, and alleviates spatial imbalances.

Overall, behavior influences not only aggregate levels, but the key factor is whether cropping patterns converge and irrigation demand becomes synchronized, thereby amplifying or buffering trade-offs among blue-water security, equity, and ecological constraints in drought years.

https://doi.org/10.5194/egusphere-2026-2016
Preprint. Discussion started: 10 July 2026

3.3 Spatiotemporal Evolution and Trade-off Analysis under alternative Management Scenarios

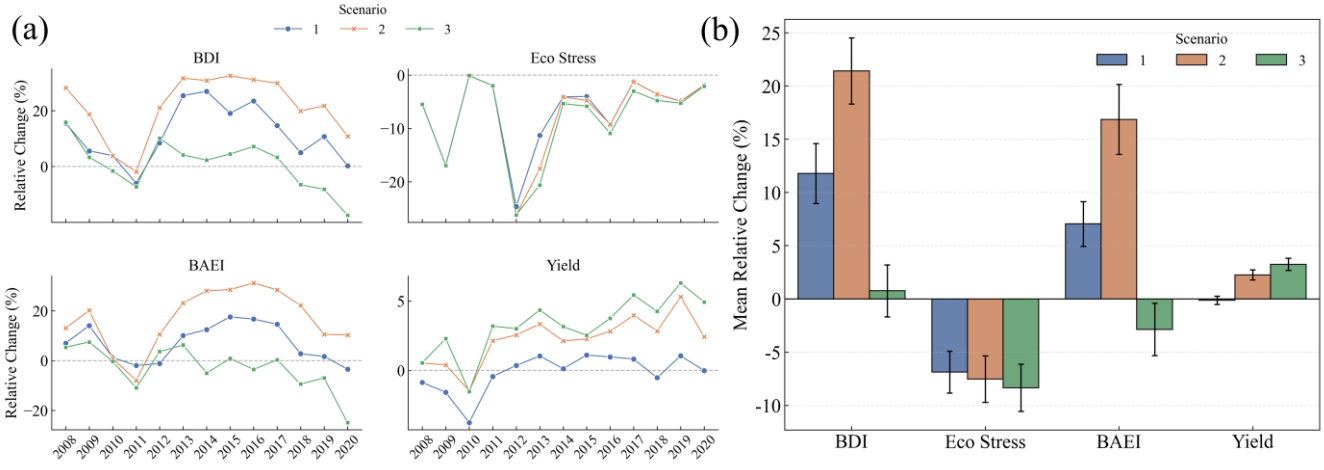

Figure 8: Figure 8. Performance trajectories and mean effects of the three management portfolios relative to the baseline. (a) Interannual relative changes (%) in basin-scale blue-water security (BDI), ecological stress (WSIeco), allocation equity (BAEI), and crop yield (Yield) for management Scenarios 1–3 compared with the baseline over 2008–2020. (b) Mean relative changes across the simulation period for each metric, with error bars showing the standard error (SE) of the interannual mean.

The three management scenarios exhibit distinct interannual fluctuation patterns over the simulation period, with the clearest contrasts occurring during the hydroclimatic perturbation window of 2010–2012 (Fig. 8a). Overall, all three scenarios reduce ecological stress to some extent by increasing effective water supply capacity, but they diverge markedly in socioeconomic performance, particularly equity, indicating that policy instruments do not generate uniform adaptive responses. The combined strategy of supply augmentation and efficiency improvement (M2) produces a comparatively smooth trajectory: although BAEI declines briefly in 2011 (−7.98%), it remains within a positive improvement range of roughly 10%–30% in subsequent years. In contrast, coupling supply augmentation with price regulation (M3) yields substantially stronger interannual volatility in equity outcomes: BAEI decreases by 10.96% in 2011 and reaches its lowest value in 2020 (−24.94%). This contrast suggests that, relative to cost-signal-based regulation, technology-oriented efficiency improvements are more likely to sustain a stable social response during hydrologic disturbances, thereby reducing sensitivity of system performance to external variability.

Aggregate performance statistics further reveal structural differences among policy tools in the efficiency–equity–production space (Fig. 8b). M2 achieves the largest improvements in both basin-scale blue-water security (BDI) and allocation equity (BAEI), with mean relative increases of 21.41% and 16.86%, respectively, indicating a strong synergistic effect in enhancing supply reliability while alleviating spatial imbalances. M3 delivers the highest mean increase in grain yield (3.25%), but this gain is accompanied by a decline in equity (mean −2.87%), reflecting a clear trade-off between production enhancement and equity maintenance. By comparison, the supply-only scenario (M1) increases BDI by 11.78% on average, yet produces a slight decrease in grain yield (mean −0.13%). This result implies that, without complementary measures such as efficiency improvements or behavioral/economic constraints, additional supply is more likely to be absorbed by demand catch-up and may not translate into sustained yield gains.

https://doi.org/10.5194/egusphere-2026-2016
Preprint. Discussion started: 10 July 2026

4 Discussion

4.1 From Farmer Decisions to Basin Responses: Mechanisms and Transferable Insights

Using the coupled SWAT–ABM framework, we show how interactions between heterogeneous farmer decisions and management interventions reshape blue–green water use, the triggering of ecological constraints, and spatial patterns of equity within an irrigation district. A central finding is that system vulnerability is not determined solely by "how much water is available," but also by whether micro-level decisions induce basin-scale temporal synchronization of irrigation demand and spatial concentration of withdrawals, thereby creating cross-scale human–water feedbacks(Di Baldassarre et al., 2019; Van Loon et al., 2016). Under the same climatic forcing and engineering boundary conditions, different decision tendencies can substantially alter peak irrigation demand, blue-water extraction intensity, and the frequency of ecological flow deficits, leading to divergent pathways ranging from "higher output with higher hydrologic risk" to "more stable output with stronger buffering capacity."

The contrast between S8 and S7 illustrates how differences in decision rules propagate through a "cropping structure–demand timing–extraction peaks" pathway to amplify or dampen drought impacts. Under a stronger profit-oriented tendency, farmers in S8 converge toward a single high-return crop (maize reaching 98.4% in 2019), which increases the overlap of water demand during critical growth stages and strengthens basin-scale aggregation of withdrawals. This demand synchronization elevates dry-year peak blue-water withdrawals and compresses system safety margins, making irrigation deficits and ecological flow constraints more likely to be triggered and resulting in sharp performance deterioration in drought years. By contrast, the diversity maintained in S7 through social imitation and satisficing tendencies (a maize–peanut–soybean mix) partially staggers critical demand periods, reducing the temporal concentration and spatial clustering of water stress and preserving buffering capacity(Davis et al., 2018). This comparison suggests that individual-level yield or profit gains, if accompanied by basin-scale demand synchronization, can translate into system-level vulnerability via amplified peak pressure, whereas maintaining diversity in decisions and cropping patterns can reduce peak-withdrawal risk through demand staggering and dispersion.

These behavior-driven process differences also help explain why management strategies diverge in both mechanisms and social consequences. M1 (supply augmentation) raises the upper bound of irrigation-season availability, but without complementary behavioral constraints and efficiency improvements, the added water is more readily absorbed by demand catch-up: farmers tend to maintain existing irrigation habits or expand water-intensive configurations, shifting total withdrawals upward rather than substantially improving water use per unit output, consistent with diminishing marginal returns(Berbel and Mateos, 2014; Grafton et al., 2018). M3 (uniform water-price increases) changes irrigation decisions through a cost signal, but elicits heterogeneous responses across resource endowments(Schoengold, 2010): vulnerable farmers contract irrigation or adjust production sooner, whereas better-resourced farmers maintain or even intensify water use. This asymmetry can concentrate water accessibility toward advantaged units and is reflected in declining equity (mean BAEI −2.87%). In contrast, M2 (supply augmentation plus efficiency improvement) reduces water requirements per unit output and

https://doi.org/10.5194/egusphere-2026-2016
Preprint. Discussion started: 10 July 2026

weakens rigid dependence on blue-water withdrawals during critical periods, producing a smoother response during the wet-to-dry transition window (2010–2012) and lowering the risk of social differentiation that can accompany purely economic constraints. Overall, the effectiveness of management tools depends on whether they modify the process chain of "demand synchronization–peak extraction–ecological constraint triggering," rather than merely increasing supply or imposing a cost signal.

These findings provide a transferable diagnostic perspective and conditional insights for other irrigation districts. First, when a system faces strong seasonal hard constraints (rigid dry-season supply and binding ecological baseflow requirements) and crop critical water-demand periods overlap, decision or policy drivers that promote crop-structure concentration and irrigation-demand synchronization are more likely to create a risk chain in which amplified peak pressure can lead to drought-year performance collapse. This risk can be screened using indicators such as maximum crop share, crop diversity indices, the peak-to-mean ratio of irrigation withdrawals (peak/mean), and the share of withdrawals occurring in the dry season. Second, supply-side expansion, when not accompanied by behavioral constraints and efficiency improvements, often induces demand catch-up and diminishing marginal returns; therefore, supply augmentation and operational optimization are better viewed as buffers rather than stand-alone solutions. Third, where user heterogeneity is pronounced and protective mechanisms (e.g., tiered volumetric pricing or targeted subsidies) are absent, uniform price instruments are more likely to generate a structural trade-off of higher efficiency but lower equity. Price policies that aim to maintain equity should be co-designed with efficiency improvements, protection for vulnerable users, and measures that discourage spatial re-concentration of water use. Overall, sustainable transitions are more likely to rely on a combined pathway of reducing water use per unit output while suppressing demand synchronization and spatial re-concentration, rather than pursuing single-objective efficiency maximization.

4.2 Limitations and Future Research

Although this study provides useful insights into trade-offs among irrigation water-management policies, several limitations should be noted to clarify the boundary conditions of our findings. First, regarding the representation of human behavior, while the ABM includes flexible adaptive mechanisms, the decision rules primarily rely on economic rationality and a limited set of heuristics. Future work could incorporate richer socio-psychological processes—such as peer effects, evolving risk perception, and social-learning theories—to better approximate farmer behavior. Second, with respect to data uncertainty, although socioeconomic parameters were adjusted using available observations, continued long-term monitoring of farmer behavior is recommended to further calibrate and validate the behavioral module of the coupled model. Finally, in the scenario design, we examined static policy interventions (e.g., a fixed water-price increase), whereas real-world policy making is often dynamic and adaptive. Future research should explore adaptive pathways in which management strategies are adjusted in response to changing hydroclimatic conditions, thereby providing more resilient solutions for the water–ecology–food–society nexus.

https://doi.org/10.5194/egusphere-2026-2016
Preprint. Discussion started: 10 July 2026

5 Conclusions

This study developed a spatially explicit, bidirectionally coupled SWAT–ABM framework and, based on blue–green water accounting, quantitatively assessed how heterogeneous farmer decisions and management interventions jointly shape the water–ecology–food–society (WEFS) nexus in an irrigation district. Results show that system performance depends not only on the level of water supply, but also on basin-scale outcomes emergent from micro-level decisions—particularly adjustments in cropping structure, temporal synchronization of irrigation demand, and spatial concentration of withdrawals. These processes govern dry-year peak blue-water extraction, the frequency of ecological-constraint triggering, and the spatial distribution of water stress. Behavioral experiments indicate that a more profit-oriented decision tendency (S8) can increase crop output in some years, but it also drives convergence toward a single crop, intensifying demand overlap during critical growth stages and compressing system safety margins. As a consequence, drought-year blue-water deficits and equity risks are substantially amplified. In contrast, strategies dominated by social learning and satisficing tendencies (S7) maintain crop diversity and stagger water demand, creating basin-scale buffering capacity and improving robustness to hydroclimatic shocks. These results emphasize that, in irrigation districts with strong seasonal supply constraints and binding ecological flow requirements, maintaining diversity in decisions and cropping patterns can reduce the risk chain of "demand synchronization–peak extraction–constraint triggering." Policy experiments further delineate the mechanisms and trade-offs associated with different intervention tools. Supply augmentation alone (M1), without coordinated behavioral and efficiency adjustments, is readily absorbed by demand catch-up, exhibits diminishing marginal returns, and is unlikely to fundamentally resolve persistent supply–demand gaps. Water-price increases (M3) can improve allocation efficiency, but heterogeneous responses across users may promote spatial re-concentration of water accessibility, generating a structural trade-off of higher efficiency but lower equity. By comparison, combining efficiency improvements with supply support (M2) reduces water use per unit output and dampens sensitivity to precipitation deficits during wet-to-dry transitions, yielding a more robust system response. Overall, sustainable irrigation management should not rely solely on supply expansion or a single economic signal. Instead, technology-enabled efficiency gains, differentiated economic mechanisms, and behavior-oriented measures should be co-designed: improving water productivity through conservation and efficiency, while using protective measures (e.g., tiered volumetric pricing, targeted subsidies, or support for vulnerable users) to mitigate regressive impacts and discourage re-concentration of water use. Such integrated portfolios can better enhance robustness to climate uncertainty while meeting ecological constraints and equity objectives.

Code and data availability

All meteorological forcing data (precipitation, air temperature, relative humidity, solar radiation, and wind speed) were obtained from the National Meteorological Science Data Sharing Service Platform (https://data.cma.cn/). Observed streamflow records from five hydrological stations were collected from

https://doi.org/10.5194/egusphere-2026-2016
Preprint. Discussion started: 10 July 2026

the Hydrological Yearbook of the People's Republic of China, published by the Ministry of Water Resources (http://www.mwr.gov.cn/). Spatial datasets include land use data (30 m resolution) from the Resource and Environment Science and Data Center (https://www.resdc.cn/), soil properties from the Harmonized World Soil Database (HWSD) (https://www.fao.org/soils-portal/soil-survey/soil-maps-and-databases/harmonized-world-soil-database-v12/en/), and the digital elevation model from the Geospatial Data Cloud (https://www.gscloud.cn/). Socioeconomic inputs (crop benefits and costs, technology costs, and water prices) were compiled from the Cost-Benefit of Major Agricultural Products Nationwide dataset(https://www.ndrc.gov.cn/fggz/). Data used to fit crop yield–evapotranspiration relationships were obtained from the 4TU.ResearchData repository：
(https://data.4tu.nl/datasets/7b45bcc6-686b-404d-a910-13c87156716a/1)
All source code used in this study is based on publicly available software. The agent-based modeling component was implemented using the Mesa framework (https://github.com/mesa/mesa). The hydrological simulations were conducted with a re-compilable version of SWAT obtained from https://github.com/crazyzlj/SWAT. The scripts developed to couple the human–water modules and to generate the analyses and figures are available from the corresponding author upon reasonable request

Supplement link

The link to the supplement will be included by Copernicus, if applicable.

Author contributions

Y.L. designed the study, developed the model, performed the simulations, analyzed the results, and wrote the original draft. S.Z. contributed to model development and data processing. M.W. contributed to data collection and result interpretation. J.F.A. contributed to conceptualization and manuscript revision. X.C. conceived and supervised the study, contributed to interpretation of the results, and revised the manuscript. All authors discussed the results and approved the final manuscript.

Competing interests

The contact author has declared that none of the authors has any competing interests.

https://doi.org/10.5194/egusphere-2026-2016
Preprint. Discussion started: 10 July 2026

Disclaimer

Publisher's note: Copernicus Publications remains neutral with regard to jurisdictional claims in published maps and institutional affiliations.

Acknowledgements

We gratefully acknowledge the research data provided by the Yahekou Irrigation District Administration in Nanyang City, Henan Province, China. This article uses generative artificial intelligence Chatgpt to improve the grammar and fluency of the manuscript.

Financial support

This work was jointly funded by the National Natural Science Foundation of China (52479038, 52309049), the Natural Science Foundation of Jiangsu Province (BK20230969), and the Fundamental Research for the Central Universities (No. B240205046).

Review statement

The review statement will be added by Copernicus Publications listing the handling editor as well as all contributing referees according to their status anonymous or identified.

References

Abbaspour, K. C., Rouholahnejad, E., Vaghefi, S., Srinivasan, R., Yang, H., and Kløve, B.: A continental-scale hydrology and water quality model for Europe: Calibration and uncertainty of a high-resolution large-scale SWAT model, Journal of Hydrology, 524, 733–752, https://doi.org/10.1016/j.jhydrol.2015.03.027, 2015.

Alam, M. F., McClain, M., Sikka, A., and Pande, S.: Understanding human–water feedbacks of interventions in agricultural systems with agent based models: a review, Environ. Res. Lett., 17, 103003, https://doi.org/10.1088/1748-9326/ac91e1, 2022.

Albers, L. T., Schyns, J. F., Booij, M. J., and Zhuo, L.: Blue water footprint caps per sub-catchment to mitigate water scarcity in a large river basin: The case of the Yellow River in China, Journal of Hydrology, 603, 126992, https://doi.org/10.1016/j.jhydrol.2021.126992, 2021.

Berbel, J. and Mateos, L.: Does investment in irrigation technology necessarily generate rebound effects? A simulation analysis based on an agro-economic model, Agricultural Systems, 128, 25–34, https://doi.org/10.1016/j.agsy.2014.04.002, 2014.

https://doi.org/10.5194/egusphere-2026-2016
Preprint. Discussion started: 10 July 2026

Bourceret, A., Amblard, L., and Mathias, J.-D.: Adapting the governance of social–ecological systems to behavioural dynamics: An agent-based model for water quality management using the theory of planned behaviour, Ecological Economics, 194, 107338, https://doi.org/10.1016/j.ecolecon.2021.107338, 2022.

Cao, X., Zeng, W., Wu, M., Guo, X., and Wang, W.: Hybrid analytical framework for regional agricultural water resource utilization and efficiency evaluation, Agricultural Water Management, 231, 106027, https://doi.org/10.1016/j.agwat.2020.106027, 2020.

Cao, X., Bao, Y., Li, Y., Li, J., and Wu, M.: Unravelling the effects of crop blue, green and grey virtual water flows on regional agricultural water footprint and scarcity, Agricultural Water Management, 278, 108165, https://doi.org/10.1016/j.agwat.2023.108165, 2023.

Chatterjee, S., Lamba, R., and Zaveri, E. D.: The role of farm subsidies in changing India's water footprint, Nat Commun, 15, 8654, https://doi.org/10.1038/s41467-024-52858-6, 2024.

D. N. Moriasi, J. G. Arnold, M. W. Van Liew, R. L. Bingner, R. D. Harmel, and T. L. Veith: Model Evaluation Guidelines for Systematic Quantification of Accuracy in Watershed Simulations, Transactions of the ASABE, 50, 885–900, https://doi.org/10.13031/2013.23153, 2007.

Davis, K. F., Chiarelli, D. D., Rulli, M. C., Chhatre, A., Richter, B., Singh, D., and DeFries, R.: Alternative cereals can improve water use and nutrient supply in India, Science Advances, 4, eaao1108, https://doi.org/10.1126/sciadv.aao1108, 2018.

Di Baldassarre, G., Sivapalan, M., Rusca, M., Cudennec, C., Garcia, M., Kreibich, H., Konar, M., Mondino, E., Mård, J., Pande, S., Sanderson, M. R., Tian, F., Viglione, A., Wei, J., Wei, Y., Yu, D. J., Srinivasan, V., and Blöschl, G.: Sociohydrology: Scientific Challenges in Addressing the Sustainable Development Goals, Water Resources Research, 55, 6327–6355, https://doi.org/10.1029/2018WR023901, 2019.

Ding, B., Zhang, J., Zheng, P., Li, Z., Wang, Y., Jia, G., and Yu, X.: Water security assessment for effective water resource management based on multi-temporal blue and green water footprints, Journal of Hydrology, 632, 130761, https://doi.org/10.1016/j.jhydrol.2024.130761, 2024.

Du, E., Cai, X., Brozović, N., and Minsker, B.: Evaluating the impacts of farmers' behaviors on a hypothetical agricultural water market based on double auction, Water Resources Research, 53, 4053–4072, https://doi.org/10.1002/2016WR020287, 2017.

Du, E., Tian, Y., Cai, X., Zheng, Y., Li, X., and Zheng, C.: Exploring spatial heterogeneity and temporal dynamics of human-hydrological interactions in large river basins with intensive agriculture: A tightly coupled, fully integrated modeling approach, Journal of Hydrology, 591, 125313, https://doi.org/10.1016/j.jhydrol.2020.125313, 2020.

Duan, Y., Zhou, S., He, J., and Bai, M.: Improving the performance of agricultural temporary water markets: The role of technology-based and transaction-based subsidies, Agricultural Water Management, 303, 109062, https://doi.org/10.1016/j.agwat.2024.109062, 2024.

Filatova, T., Akkerman, J., Bosello, F., Chatzivasileiadis, T., Cortés Arbués, I., Ghorbani, A., Ivanova, O., Knittel, N., Kwakkel, J., Lamperti, F., Magliocca, N. R., Marangoni, G., Nabernegg, S., Pichler, A., Poujon, A., Safarzynska, K., Taberna, A., van

https://doi.org/10.5194/egusphere-2026-2016
Preprint. Discussion started: 10 July 2026

Sluisveld, M. A. E., Verbeek, L., and Wei, T.: The power of bridging decision scales: Model coupling for advanced climate policy analysis, Proceedings of the National Academy of Sciences, 122, e2411592122, https://doi.org/10.1073/pnas.2411592122, 2025.

Genova, P. and Wei, Y.: A socio-hydrological model for assessing water resource allocation and water environmental regulations in the Maipo River basin, Journal of Hydrology, 617, 129159, https://doi.org/10.1016/j.jhydrol.2023.129159, 2023.

Grafton, R. Q., Williams, J., Perry, C. J., Molle, F., Ringler, C., Steduto, P., Udall, B., Wheeler, S. A., Wang, Y., Garrick, D., and Allen, R. G.: The paradox of irrigation efficiency, Science, 361, 748–750, https://doi.org/10.1126/science.aat9314, 2018.

Grimm, V., Berger, U., Meyer, M., and Lorscheid, I.: Theory for and from agent-based modelling: Insights from a virtual special issue and a vision, Environmental Modelling & Software, 178, 106088, https://doi.org/10.1016/j.envsoft.2024.106088, 2024.

Hassan, W., Manzoor, T., and Muhammad, A.: Improving equity in demand-driven irrigation systems through a rights-preserving water allocation mechanism, Agricultural Water Management, 287, 108443, https://doi.org/10.1016/j.agwat.2023.108443, 2023.

Hoekstra, A. Y.: Green-blue water accounting in a soil water balance, Advances in Water Resources, 129, 112–117, https://doi.org/10.1016/j.advwatres.2019.05.012, 2019.

Huber, R., Späti, K., and Finger, R.: A behavioural agent-based modelling approach for the ex-ante assessment of policies supporting precision agriculture, Ecological Economics, 212, 107936, https://doi.org/10.1016/j.ecolecon.2023.107936, 2023.

James V. Miranda, L.: PySwarms: a research toolkit for Particle Swarm Optimization in Python, JOSS, 3, 433, https://doi.org/10.21105/joss.00433, 2018.

Li, Y., Wu, M., Adamowski, J. F., and Cao, X.: Blue-green water migration and utilization efficiency under various irrigation-drainage measures applied to a paddy field, Journal of Hydrology: Regional Studies, 51, 101641, https://doi.org/10.1016/j.ejrh.2023.101641, 2024.

Luan, X.-B., Yin, Y.-L., Wu, P.-T., Sun, S.-K., Wang, Y.-B., Gao, X.-R., and Liu, J.: An improved method for calculating the regional crop water footprint based on a hydrological process analysis, Hydrology and Earth System Sciences, 22, 5111–5123, https://doi.org/10.5194/hess-22-5111-2018, 2018.

Lyu, J., Mo, S., Jiang, K., and Yan, S.: Seeking a pathway towards a more sustainable human-water relationship by coupled model – From a perspective of socio-hydrology, Journal of Environmental Management, 368, 122231, https://doi.org/10.1016/j.jenvman.2024.122231, 2024.

Mialyk, O., Schyns, J. F., Booij, M. J., Su, H., Hogeboom, R. J., and Berger, M.: Water footprints and crop water use of 175 individual crops for 1990–2019 simulated with a global crop model, Sci Data, 11, 206, https://doi.org/10.1038/s41597-024-03051-3, 2024.

Mijic, A., Liu, L., O'Keeffe, J., Dobson, B., and Chun, K. P.: A meta-model of socio-hydrological phenomena for sustainable water management, Nat Sustain, 7, 7–14, https://doi.org/10.1038/s41893-023-01240-3, 2024.

https://doi.org/10.5194/egusphere-2026-2016
Preprint. Discussion started: 10 July 2026

Ng, T. L., Wayland Eheart, J., Cai, X., Braden, J. B., and Czapar, G. F.: Agronomic and Stream Nitrate Load Responses to Incentives for Bioenergy Crop Cultivation and Reductions of Carbon Emissions and Fertilizer Use, J. Water Resour. Plann. Manage., 140, 112–120, https://doi.org/10.1061/(ASCE)WR.1943-5452.0000320, 2014.

Nouri, A., Saghafian, B., Delavar, M., and Bazargan-Lari, M. R.: Agent-Based Modeling for Evaluation of Crop Pattern and Water Management Policies, Water Resour Manage, 33, 3707–3720, https://doi.org/10.1007/s11269-019-02327-3, 2019.

Nozari, S., Bailey, R. T., Rad, M. R., Smith, G. E. B., Andales, A. A., Zambreski, Z. T., Tavakoli-Kivi, S., Sharda, V., Kisekka, I., Gowda, P., and Schipanski, M. E.: An integrated modeling approach to simulate human-crop-groundwater interactions in intensively irrigated regions, Environmental Modelling & Software, 179, 106120, https://doi.org/10.1016/j.envsoft.2024.106120, 2024.

Qi, X., Feng, K., Sun, L., Zhao, D., Huang, X., Zhang, D., Liu, Z., and Baiocchi, G.: Rising agricultural water scarcity in China is driven by expansion of irrigated cropland in water scarce regions, One Earth, 5, 1139–1152, https://doi.org/10.1016/j.oneear.2022.09.008, 2022.

Schoengold, K.: Irrigation Water Pricing: The Gap Between Theory and Practice, Am. J. Agr. Econ., 92, 1497–1498, https://doi.org/10.1093/ajae/aaq095, 2010.

Scott, C. A., Vicuña, S., Blanco-Gutiérrez, I., Meza, F., and Varela-Ortega, C.: Irrigation efficiency and water-policy implications for river basin resilience, Hydrol. Earth Syst. Sci., 18, 1339–1348, https://doi.org/10.5194/hess-18-1339-2014, 2014.

Seigerman, C. K., McKay, S. K., Basilio, R., Biesel, S. A., Hallemeier, J., Mansur, A. V., Piercy, C., Rowan, S., Ubiali, B., Yeates, E., and Nelson, D. R.: Operationalizing equity for integrated water resources management, J American Water Resour Assoc, 59, 281–298, https://doi.org/10.1111/1752-1688.13086, 2023.

Sousa, D. S., Silva, E. P., Alves, C. de M. A., Minoti, R. T., and Vergara, F. E.: Coupling data-driven agent-based and hydrological modelling to explore the effect of collective water allocation strategies in environmental flows, Journal of Hydrology, 652, 132670, https://doi.org/10.1016/j.jhydrol.2025.132670, 2025.

Tuninetti, M., Tamea, S., D'Odorico, P., Laio, F., and Ridolfi, L.: Global sensitivity of high-resolution estimates of crop water footprint, Water Resources Research, 51, 8257–8272, https://doi.org/10.1002/2015WR017148, 2015.

Van Loon, A. F., Stahl, K., Di Baldassarre, G., Clark, J., Rangecroft, S., Wanders, N., Gleeson, T., Van Dijk, A. I. J. M., Tallaksen, L. M., Hannaford, J., Uijlenhoet, R., Teuling, A. J., Hannah, D. M., Sheffield, J., Svoboda, M., Verbeiren, B., Wagener, T., and Van Lanen, H. A. J.: Drought in a human-modified world: reframing drought definitions, understanding, and analysis approaches, Hydrology and Earth System Sciences, 20, 3631–3650, https://doi.org/10.5194/hess-20-3631-2016, 2016.

Wens, M., Veldkamp, T. I. E., Mwangi, M., Johnson, J. M., Lasage, R., Haer, T., and Aerts, J. C. J. H.: Simulating Small-Scale Agricultural Adaptation Decisions in Response to Drought Risk: An Empirical Agent-Based Model for Semi-Arid Kenya, Front. Water, 2, https://doi.org/10.3389/frwa.2020.00015, 2020.

https://doi.org/10.5194/egusphere-2026-2016
Preprint. Discussion started: 10 July 2026

Wescoat Jr., J. L., Siddiqi, A., and Muhammad, A.: Socio-Hydrology of Channel Flows in Complex River Basins: Rivers, Canals, and Distributaries in Punjab, Pakistan, Water Resources Research, 54, 464–479, https://doi.org/10.1002/2017WR021486, 2018.

Wu, M., Li, Y., Xiao, J., Guo, X., and Cao, X.: Blue, green, and grey water footprints assessment for paddy irrigation-drainage system, Journal of Environmental Management, 302, 114116, https://doi.org/10.1016/j.jenvman.2021.114116, 2022.

Xiong, L., Xu, X., Ren, D., Huang, Q., and Huang, G.: Enhancing the capability of hydrological models to simulate the regional agro-hydrological processes in watersheds with shallow groundwater: Based on the SWAT framework, Journal of Hydrology, 572, 1–16, https://doi.org/10.1016/j.jhydrol.2019.02.043, 2019.

Xu, X., Jiang, Y., Liu, M., Huang, Q., and Huang, G.: Modeling and assessing agro-hydrological processes and irrigation water saving in the middle Heihe River basin, Agricultural Water Management, 211, 152–164, https://doi.org/10.1016/j.agwat.2018.09.033, 2019.

Yin, J., Li, X., Engel, B. A., Ding, J., Xing, X., Sun, S., and Wang, Y.: Inter-Regional Food-Water-Income Synergy Through Bi-Level Crop Redistribution Model Coupled With Virtual Water: A Case Study of China's Hetao Irrigation District, Water Resources Research, 60, e2023WR036572, https://doi.org/10.1029/2023WR036572, 2024.

Yoon, J., Klassert, C., Selby, P., Lachaut, T., Knox, S., Avisse, N., Harou, J., Tilmant, A., Klauer, B., Mustafa, D., Sigel, K., Talozi, S., Gawel, E., Medellín-Azuara, J., Bataineh, B., Zhang, H., and Gorelick, S. M.: A coupled human–natural system analysis of freshwater security under climate and population change, Proc. Natl. Acad. Sci. U.S.A., 118, e2020431118, https://doi.org/10.1073/pnas.2020431118, 2021.

Yoon, J., Voisin, N., Klassert, C., Thurber, T., and Xu, W.: Representing farmer irrigated crop area adaptation in a large-scale hydrological model, Hydrology and Earth System Sciences, 28, 899–916, https://doi.org/10.5194/hess-28-899-2024, 2024.

Yuan, S., Li, X., and Du, E.: Effects of farmers' behavioral characteristics on crop choices and responses to water management policies, Agricultural Water Management, 247, 106693, https://doi.org/10.1016/j.agwat.2020.106693, 2021.

Zhuo, L., Mekonnen, M. M., and Hoekstra, A. Y.: Sensitivity and uncertainty in crop water footprint accounting: a case study for the Yellow River basin, Hydrology and Earth System Sciences, 18, 2219–2234, https://doi.org/10.5194/hess-18-2219-2014, 2014.

Zhuo, L., Mekonnen, M. M., Hoekstra, A. Y., and Wada, Y.: Inter- and intra-annual variation of water footprint of crops and blue water scarcity in the Yellow River basin (1961–2009), Advances in Water Resources, 87, 29–41, https://doi.org/10.1016/j.advwatres.2015.11.002, 2016.

Zhuo, L., Li, M., Zhang, G., Mekonnen, M. M., Hoekstra, A. Y., Wada, Y., and Wu, P.: Volume versus value of crop-related water footprints and virtual water flows: A case study for the Yellow River Basin, Journal of Hydrology, 608, 127674, https://doi.org/10.1016/j.jhydrol.2022.127674, 2022.